

Case Report

# Malignant pinealoma observed in the deep cerebral parenchyma of a male Wistar rat

Mizuho Takagi<sup>1\*</sup>, Yuko Yamaguchi<sup>1</sup>, Seiki Yamakawa<sup>1</sup>, and Kazutoshi Tamura<sup>1</sup>

<sup>1</sup> Pathology Division, BoZo Research Center Inc., 1284 Kamado, Gotemba-shi, Shizuoka 412-0039, Japan

**Abstract:** This report describes a case of spontaneous malignant pinealoma in a 90-week-old male Wistar rat. The tumor mass occurred in the deep cerebral parenchyma and no intact pineal gland was observed in the area between the posterior-dorsal median line of the cerebrum and the cerebellum. The tumor was characterized by a large nodular proliferation occupying the central area of the brain, extending from the dorsal surface to the base of the brain, corresponding to the thalamus. The tumor cells had round to irregular oblong nuclei approximately 5–17  $\mu\text{m}$  in diameter and showed faintly or moderately eosinophilic cytoplasm and indistinct cell boundaries. Immunohistochemically, the tumor cells were positive for synaptophysin and partially positive for neuron-specific enolase (NSE). The tumor showed malignant features including cellular pleomorphism, high mitotic index, necrotic foci, and invasive and extensive growth and was, therefore, diagnosed as an extremely rare malignant pinealoma in the deep cerebral parenchyma. (DOI: 10.1293/tox.2021-0047; J Toxicol Pathol 2022; 35: 117–121)

**Key words:** pinealoma, rat, Wistar, synaptophysin, pineal gland

Pinealomas are rare tumors in humans and animals, including laboratory rats<sup>1–4</sup>. In humans, this tumor originates from the pineal cells of the pineal gland and is classified into three types: pinealoma, pineal parenchymal tumor of intermediate differentiation, and pineoblastoma<sup>5,6</sup>. Another type of tumor, germinoma, is derived from embryonal cells in the pineal region<sup>1,6</sup>. Germinoma, formerly called pinealoma, has a unique feature showing two cell patterns composed of large tumor cells and small infiltrated lymphocytes<sup>6</sup>. In addition, papillary tumors in the pineal region are listed as a very rare tumor in the 2007 and 2016 World Health Organization (WHO) tumor classifications<sup>5,7</sup>. In contrast, the tumor classification of rodent species generally classifies tumors occurring in the pineal region as pinealoma, and those with high histological grade referred to as malignant pinealoma<sup>4,8</sup>. Pinealomas derived from parenchymal cells of the pineal gland have been reported in various strains of rats, including Sprague-Dawley<sup>9</sup>, F344<sup>10,11</sup>, Wistar<sup>12–14</sup>, and Osborne Mendel<sup>15</sup> rats, and are characterized by an expansive growth of tumor cells in the area between the posterior-dorsal median line of the cerebrum and the cerebellum, where

the pineal gland is located. In rats, the highest incidence of spontaneous pinealomas (1%) has been reported in Wistar rats<sup>14</sup>; however, the incidence in other reports is generally lower<sup>10,12,15</sup>. Moreover, there are no reports in the literature on germinoma in the pineal region of rats<sup>4,16</sup>. This case report describes a malignant pinealoma showing invasive growth of tumor cells into the deep brain.

The animal was a male Wistar Hannover (RccHan: WIST) rat (Japan Laboratory Animals Inc., Kanagawa, Japan) that had served as a monitor for a safety assessment study and was found dead at 90 weeks of age. In this study, two rats of the same sex were housed in a plastic solid floor cage (440 mm  $\times$  275 mm  $\times$  180 mm) in an animal room maintained at  $23 \pm 3^\circ\text{C}$  and of  $50 \pm 20\%$  relative humidity under a 12-hour light/dark cycle. A pelleted CR-LPF diet (radiation sterilized, Oriental Yeast Co., Ltd., Tokyo, Japan) and tap water were provided *ad libitum*. All experimental procedures were conducted according to the guidelines for the control and welfare of experimental animals specified by the test facility (Rules of the Animal Experiment Committee, BoZo Research Center Inc.).

Necropsy revealed a swollen brain and no intact pineal gland in the area between the posterior-dorsal median line of the cerebrum and the cerebellum. Instead, the tumor mass protruded into this area. No gross findings were observed in the other organs. After fixation in 10% phosphate-buffered formalin, the brain was cut transversally into six separate portions. In the section passing through the pineal region, a 15  $\times$  15 mm yellowish-brown mass was observed from the upper dorsal surface of the brain to the thalamus (Fig. 1). Six sections were embedded, sectioned, and

Received: 4 August 2021, Accepted: 2 November 2021

Published online in J-STAGE: 25 November 2021

\*Corresponding author: M Takagi

(e-mail: takagi-mizuho@bozo.co.jp)

©2022 The Japanese Society of Toxicologic Pathology

This is an open-access article distributed under the terms of the

Creative Commons Attribution Non-Commercial No Derivatives

(by-nc-nd) License. (CC-BY-NC-ND 4.0: <https://creativecommons.org/licenses/by-nc-nd/4.0/>).



stained with hematoxylin and eosin (HE) and silver impregnation. Immunohistochemical staining was also performed using antibodies against synaptophysin (NICHIREI, Tokyo, Japan), NSE (NICHIREI), ED-1 (Serotec, Sapporo, Japan), Iba-1 (WAKO, Osaka, Japan), GFAP (Abcam, Cambridge, UK), Olig2 (IBL, Fujioka, Japan), vimentin (Santa Cruz, Santa Cruz, USA), S-100 (Dako, Tokyo, Japan), and nestin (Santa Cruz) for differential diagnoses<sup>17</sup>.

Histologically, the tumor was characterized by a large nodular proliferation occupying the central area of the brain, extending from the dorsal surface to the base of the brain, corresponding to the thalamus-pons, and also compressed the posterior cerebral hemispheres on both sides (Fig. 2B-d, e). In the anterior sections, the third and lateral ventricles located in the anterior area of the tumor mass were moderately dilated (Fig. 2B-a, b). In the posterior section, tumor cells were present in the fourth ventricle (Fig. 2B-f). The tumor cells were arranged in sheets and divided into incomplete lobules or nests by fibrovascular septa (Fig. 3A). The nuclei of the tumor cells varied in size, ranging from approximately 5 to 17  $\mu\text{m}$  in diameter and in shape from round, oval to irregular oblong, and contained multifocal condensed chromatin and some nucleoli (Fig. 3B). The nuclear membrane was distinct for its condensed chromatin, and smaller nuclei of the tumor cells tended to contain richer chromatin within the nuclei of the tumor cells. The cytoplasm was faintly or moderately eosinophilic and the cell boundaries were indistinct. The tumor cells showed mild pleomorphism in the cell size and nucleus shape, but no giant or multinucleated cells were present (Fig. 3B). The tumor cells had 1–23 mitotic figures per high-power field, with remarkably high mitotic activity in some areas. Several hemorrhagic and necrotic foci, including coagulation necrosis, were present in the deeper regions of the mass, with the necrotic tumor cells showing karyopyknosis (Fig. 3C). Tumor cells in the peripheral area of the tumor had invaded the brain parenchyma, with a clear

border between the tumor and normal tissues, and occasionally forming solitary islands nearby, but no fibrous capsule (Fig. 3D). Pseudo-rosettes around the blood vessel or cyst-like structures containing eosinophilic liquid material were occasionally observed, although no true rosettes were noted (Fig. 3E). On silver impregnation, the tumor cells were incompletely compartmentalized into various sizes of nests by argentaffin fibers (Fig. 3F). Immunohistochemical analysis revealed that the tumor cells were positive for synaptophysin (Fig. 4A) and partially positive for NSE (Fig. 4B). In contrast, the tumor cells were negative for ED-1, Iba-1, GFAP, Olig2, vimentin, S-100, and nestin (Table 1). A small

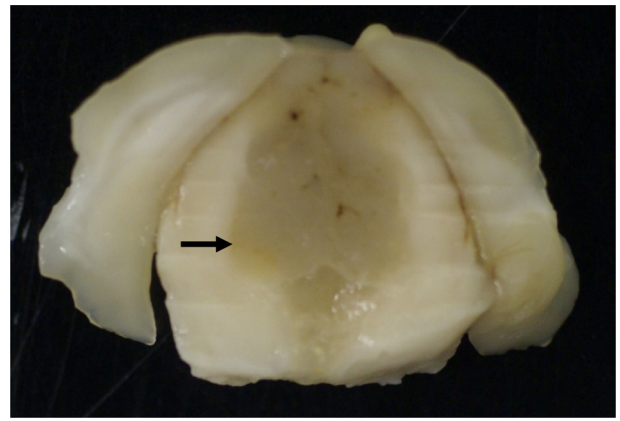


**Fig. 1.** Macroscopic features of the tumor in the transversal cut surface of the formalin-fixed brain passing through the location where the pineal gland is normally present. A yellowish-brown mass occupies the central area of the brain, extending from the dorsal surface to the base of the brain corresponding to the thalamus-pons, and expands from the cerebral median line to both sides of the brain stem. The arrow indicates the border between the tumor and brain parenchyma.

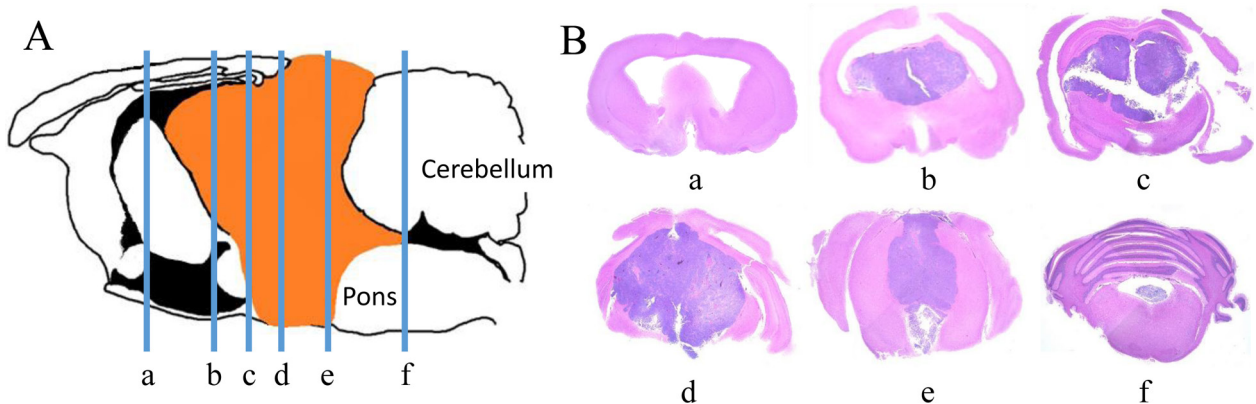


**Fig. 2.** (A) Schematic view of the tumor (filled with orange color) in a longitudinal median plane of the brain. The areas filled with black color indicate the dilated ventricles. The blue bar (a–f) indicates the anatomical location where the specimen was prepared. (B) Low-magnification images of each histological specimen stained with hematoxylin and eosin (HE) (a–f). The tumor mass extends from the region where the pineal gland is normally present to the thalamus (d) and pons (e). The mass is invading the third and lateral ventricles and reaches the fourth ventricle (b–f). The third and lateral ventricles in the anterior area of the tumor are moderately dilated (a, b).

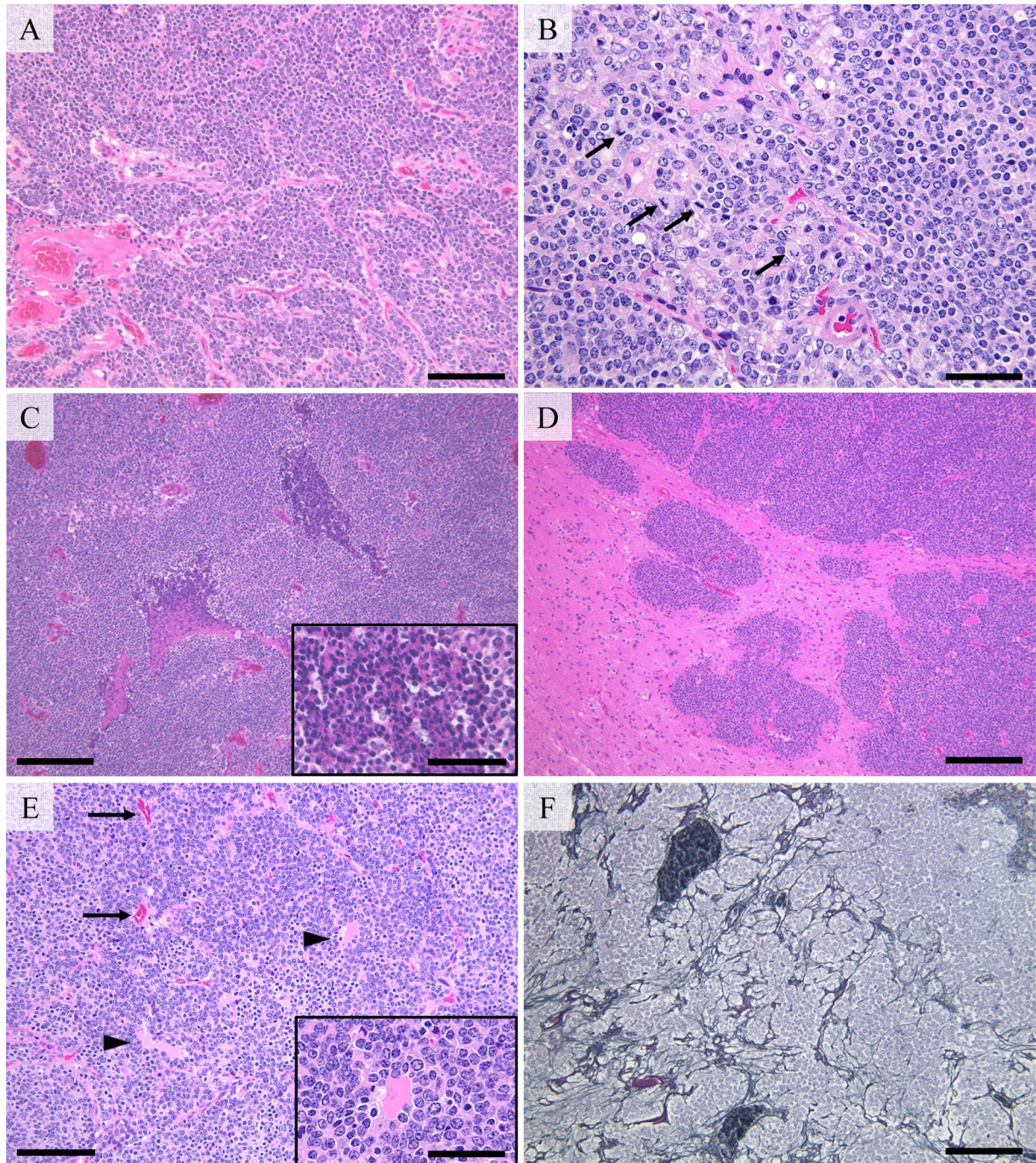


**Fig. 3.** (A) Tumor cells arranged in sheets and partially compartmentalized by fibrous connective tissues into incomplete lobules or nests. Hematoxylin and eosin (HE). Bar=100  $\mu$ m. (B) Tumor cells of varying size and shape, with round, oval, or irregular oblong nuclei and faintly eosinophilic cytoplasm with indistinct boundaries. The smaller nuclei of the tumor cells contain richer chromatin. Mitotic figures (arrows) are frequent. HE. Bar=50  $\mu$ m. (C) Large necrotic areas with coagulation necrosis are present within the tumor. The necrotic tumor cells show karyopyknosis. HE. Bar=200  $\mu$ m. The inset shows a higher-power view of the necrotic tumor cells with karyopyknosis. Bar=50  $\mu$ m. (D) At the margins of the tumor mass, tumor cells invade the brain parenchyma and form island-like nests. HE. Bar=200  $\mu$ m. (E) Pseudo-rosette formation around the blood vessels (arrows) and cyst-like structures containing eosinophilic liquid material (arrowheads). HE. Bar=100  $\mu$ m. The inset shows a higher-power view of the pseudo-rosette. Bar=50  $\mu$ m. (F) Tumor cells incompletely compartmentalized into various sizes of nests accompanied by blood vessels by argentaaffin fibers. Silver impregnation. Bar=100  $\mu$ m.

number of GFAP-positive reactive astrocytes were observed at the border between the tumor and normal tissues. Based on these results, the tumor cell was determined to originate from the pineal parenchymal cells and was, thus, diagnosed as a malignant pinealoma affecting the deep brain parenchyma.

In rats, pinealomas occur at a typical location between the cerebral hemispheres and the cerebellum, where the pineal gland is located<sup>4, 8</sup>. The expansive growth of tumor cells in the dorsal surface of the brain is also a biological feature of pinealomas in rats, even when the tumor is malignant<sup>8</sup>. In previous reports, the tumor masses were visible on the dorsal surface of the brain<sup>9, 11-14</sup>. However, unlike these previous reports of spontaneous pinealomas in rats, the present tumor occurred in the deep brain parenchyma and grew to a large mass invading the brain parenchyma. The rat pineal gland at the dorsal pineal region is anatomically connected to the roof of the diencephalon by a long slender stalk, and pineal cells still exist in the pineal stalk of young rats<sup>8, 11, 18</sup>. Therefore, the abnormal location of the present tumor suggested that the tumor occurred at the stalk of the pineal gland in the deep brain parenchyma.

In humans, germinoma, formerly called pinealoma, has a unique feature of two cell patterns composed of large tumor cells and small infiltrated lymphocytes<sup>6</sup>. In contrast,

pinealomas in rats derived from parenchymal cells of the pineal gland are reportedly composed of large and small tumor cells<sup>9, 10, 12, 13</sup>. The histopathological features and cellular morphology of the present case were similar to those of pinealomas in rats reported previously<sup>9-15</sup>. Cellular pleomorphism is a common feature of pinealomas, especially malignant tumors<sup>11, 13, 14</sup>. Furthermore, the presence of giant cells such as gigantic or multinucleated cells<sup>9</sup>, tumor cells with gigantic nuclei<sup>13</sup>, and giant or multinucleated cells<sup>14</sup> have been reported in pinealomas of rats. The tumor cells in the present case showed mild pleomorphism in cell size and nuclei shape, with a lack of giant cells and were not regarded as evidence of the tumor consisting of two cell types, although pinealomas in rats showed two cell patterns consisting of large and small-sized cells<sup>9, 10, 12, 13</sup>.

The tumor in the present case grew invasively and extensively into the brain parenchyma, with necrosis and hemorrhage observed in many areas within the tumor. In addition, tumor cells displayed numerous mitotic figures. These features indicated that the tumor was malignant. Immunohistochemistry showed that the tumor cells were positive for synaptophysin and NSE but negative for GFAP, S-100, and vimentin, findings similar to those reported previously in pinealomas in rats<sup>11, 14</sup>. Combined, the findings mentioned above strongly indicated that the tumor was a malignant

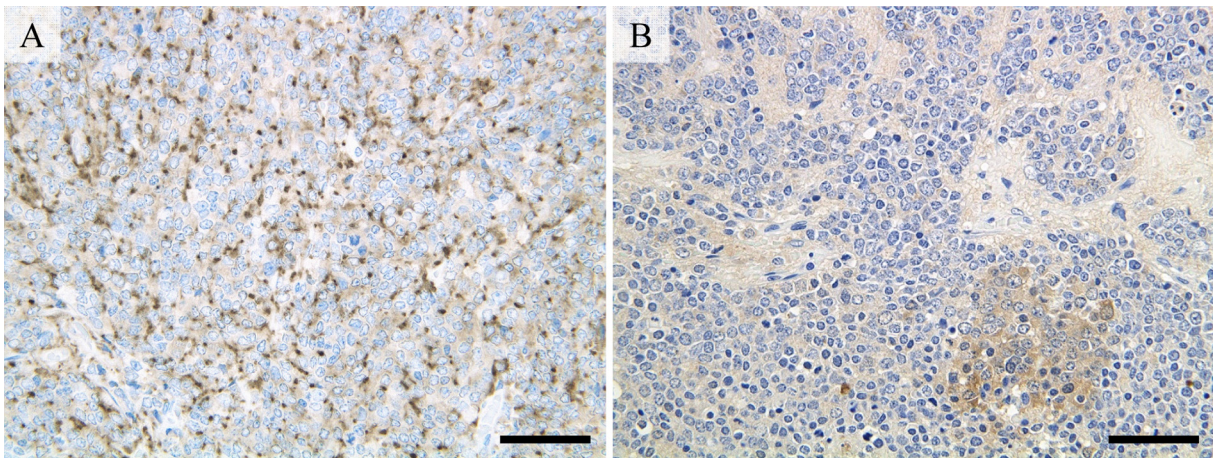


**Fig. 4.** (A) The cytoplasm of most tumor cells is positive for synaptophysin. Immunohistochemistry for synaptophysin. Bar=50  $\mu$ m. (B) The tumor cells are partially positive for neuron-specific enolase (NSE). Positive staining is visible in a small focus comprising tumor cells with relatively large nuclei. Immunohistochemistry for NSE. Bar=50  $\mu$ m.

**Table 1.** Immunohistochemical Stainability on the Present Tumor and Other Intracranial Tumors Described in the Literature

Primary antibody	NSE	Synaptophysin	ED-1	Iba-1	GFAP	S-100	Vimentin	Olig2	Nestin
Present case	+/-	+	-	-	-	-	-	-	-
Pinealoma	+/-	+				-	-		
Ependymoma					+/-		+		
Oligodendroglioma					-/+		-	+	-
Astrocytoma			+	+	-/+		+		+/-
Medulloblastoma	N	N	N	N	N	N	N	N	N

-, negative; +, positive; N, no specific immunohistochemical markers were identified.

pinealoma. Regarding the differential diagnoses, ependymoma, oligodendroglioma, and astrocytoma were ruled out based on the negative staining for ED-1, Iba-1, GFAP, vimentin, Olig2, and nestin (Table 1)<sup>4, 8, 19–21</sup>. In addition, the extensive invasive growth of the present tumor in both the cerebrum and cerebellum differed from the growth pattern of medulloblastoma, which develops in the cerebellum.

In conclusion, we described an extremely rare case of malignant pinealomas in the rat that probably originated from the stalk of the pineal gland<sup>18</sup> in the deep cerebral parenchyma. Further studies are necessary to clarify the pathogenesis of this tumor.

**Disclosure of Potential Conflicts of Interest:** The authors declare that they have no conflicts of interest.

**Acknowledgments:** We are grateful to Dr. Kunitoshi Mitsumori, Professor Emeritus of the Tokyo University of Agriculture and Technology, for his critical review of this manuscript. We are also grateful to Dr. Ryo Ando at the Department of Veterinary Medicine, Kitasato University, for his technical assistance with anti-synaptophysin staining and Pete Aughton, BSc, DipRCPath, DABT, at the ITR Laboratories Canada, for English language editing.

## References

- Maitra A. The endocrine system. In: Robbins and Cotran Pathologic Basis of Disease, 9th ed. V Kumar, AK Abbas, and JC Aster (eds). Elsevier, Philadelphia. 1073–1139. 2015.
- La Perle KMD. Endocrine system. In: Pathologic Basis of Veterinary Disease, 5th ed. JF Zachary, and MD McGavin (eds). Mosby, St Louis. 660–697. 2012.
- Higgins RJ, Bollen AW, Dickinson PJ, and Siso-Llonch S. Tumors of the nervous system. In: Tumors in Domestic Animals, 5th ed. Meuten DJ (ed). Wiley-Blackwell, Raleigh. 834–891. 2017.
- Weber K, Garman RH, Germann PG, Hardisty JF, Krinke G, Millar P, and Pardo ID. Classification of neural tumors in laboratory rodents, emphasizing the rat. *Toxicol Pathol.* **39**: 129–151. 2011. [[Medline](#)] [[CrossRef](#)]
- Louis DN, Perry A, Reifenberger G, von Deimling A, Figarella-Branger D, Cavenee WK, Ohgaki H, Wiestler OD, Kleihues P, and Ellison DW. The 2016 World Health Organization Classification of Tumors of the Central Nervous System: a summary. *Acta Neuropathol.* **131**: 803–820. 2016. [[Medline](#)] [[CrossRef](#)]
- Sasaki A. Pathological diagnosis of the pineal region tumors. *Progress in Neuro Oncol.* **21**: 1–8. 2014 (in Japanese).
- Louis DN, Ohgaki H, Wiestler OD, Cavenee WK, Burger PC, Jouvet A, Scheithauer BW, and Kleihues P. The 2007 WHO classification of tumours of the central nervous system. *Acta Neuropathol.* **114**: 97–109. 2007. [[Medline](#)] [[CrossRef](#)]
- Brändli-Baiocco A, Balme E, Bruder M, Chandra S, Hellmann J, Hoenerhoff MJ, Kambara T, Landes C, Lenz B, Mense M, Rittinghausen S, Satoh H, Schorsch F, Seeliger F, Tanaka T, Tsuchitani M, Wojcinski Z, and Rosol TJ. Non-proliferative and Proliferative Lesions of the Rat and Mouse Endocrine System. *J Toxicol Pathol.* **31**(Suppl): 1S–95S. 2018. [[Medline](#)] [[CrossRef](#)]
- Furukawa S, Kobayashi K, Usuda K, Tamura T, Miyamoto Y, Hayashi K, Ikeyama S, Goryo M, and Okada K. Spontaneous pinealoma in a male Crj:CD (SD) IGS rat. *J Vet Med Sci.* **61**: 41–44. 1999. [[Medline](#)] [[CrossRef](#)]
- Maekawa A, Onodera H, Tanigawa H, Furuta K, Takahashi M, Kurokawa Y, Kokubo T, Ogiu T, Uchida O, Kobayashi K, and Hayashi Y. Spontaneous tumors of the nervous system and associated organs and/or tissues in rats. *Gan.* **75**: 784–791. 1984. [[Medline](#)]
- Heath JE, and Winokur TS. Case report: pineocytoma in a male Fischer 344 rat. *Toxicol Pathol.* **26**: 294–297. 1998. [[Medline](#)] [[CrossRef](#)]
- Al Zubaidy AJ, and Malinowski W. Spontaneous pineal body tumours (pinealomas) in Wistar rats; a histological and ultrastructural study. *Lab Anim.* **18**: 224–229. 1984. [[Medline](#)] [[CrossRef](#)]
- Yamamoto O, Mitsumori K, Yoshida T, Maita K, and Shirasu Y. Spontaneous malignant pineocytoma in a female Wistar rat. *J Vet Med Sci.* **53**: 527–529. 1991. [[Medline](#)] [[CrossRef](#)]
- Treumann S, Buesen R, Gröters S, Eichler JO, and van Ravenzwaay B. Occurrence of pineal gland tumors in combined chronic toxicity/carcinogenicity studies in Wistar rats. *Toxicol Pathol.* **43**: 838–843. 2015. [[Medline](#)] [[CrossRef](#)]
- Dagle GE, Zwicker GM, and Renne RA. Morphology of spontaneous brain tumors in the rat. *Vet Pathol.* **16**: 318–324. 1979. [[Medline](#)] [[CrossRef](#)]
- Koestner A, and Solleveld HA. Tumors of the pineal gland, rat. In: Monographs on Pathology of Laboratory Animals, Endocrine System, 2nd ed., TC Jones, CC Capen, and U Mohr (eds). Springer Verlag, Berlin. 205–213. 1996.
- Moroki T, Matsuo S, Hatakeyama H, Hayashi S, Matsumoto I, Suzuki S, Kotera T, Kumagai K, and Ozaki K. Databases for technical aspects of immunohistochemistry: 2021 update. *J Toxicol Pathol.* **34**: 161–180. 2021. [[Medline](#)] [[CrossRef](#)]
- Calvo J, and Boya J. Postnatal evolution of the rat pineal gland: light microscopy. *J Anat.* **138**: 45–53. 1984. [[Medline](#)]
- Adams ET, Auerbach S, Blackshear PE, Bradley A, Gruebel MM, Little PB, Malarkey D, Maronpot R, McKay JS, Miller RA, Moore RR, Morrison JP, Nyska A, Ramot Y, Rao D, Suttie A, Wells MY, Willson GA, and Elmore SA. Proceedings of the 2010 National Toxicology Program Satellite Symposium. *Toxicol Pathol.* **39**: 240–266. 2011. [[Medline](#)] [[CrossRef](#)]
- Bradley A, Bertrand L, Rao DB, Hall DG, and Sharma AK. Brain. In: Boorman's Pathology of the Rat. Reference and Atlas, 2th ed. AW Suttie, JR Leininger, and AE Bradley (eds). Academic Press, Cambridge. 191–215. 2018.
- Nagatani M, Yamakawa S, Saito T, Ando R, Hoshiya T, Tamura K, and Uchida K. GFAP-positive neoplastic astrocytes in spontaneous oligodendrogliomas and mixed gliomas of rats. *Toxicol Pathol.* **41**: 653–661. 2013. [[Medline](#)] [[CrossRef](#)]